

A MIXTURE-OF-EXPERTS FRAMEWORK WITH LOG-LOGISTIC COMPONENTS FOR SURVIVAL ANALYSIS ON HISTOPATHOLOGY IMAGES

Ardhendu Sekhar, Vasu Soni, Keshav Aske, Shivam Madnoorkar, Pranav Jeevan, Amit Sethi

Indian Institute of Technology Bombay

ABSTRACT

We propose a modular framework for predicting cancer-specific survival from whole-slide pathology images (WSIs). The method integrates four components: (i) Quantile-Gated Patch Selection via quantile-based thresholding to isolate prognostically informative tissue regions; (ii) Graph-Guided Clustering using k -NN graph to capture phenotype-level heterogeneity through spatial-morphological coherence; (iii) Hierarchical Context Attention to learn intra- and inter-cluster interactions; and (iv) an Expert-Driven Mixture of Log-logistics framework to estimate complex survival distributions using Log-logistics distributions. The model attains a concordance index of 0.644 ± 0.059 on TCGA-LUAD, 0.751 ± 0.037 on TCGA-KIRC, and 0.752 ± 0.011 on TCGA-BRCA, respectively, outperforming existing state-of-the-art approaches.

Index Terms— Survival Analysis, Whole-Slide Images, Histopathology, Attention, Mixture of Experts, Deep Learning.

1. INTRODUCTION

Accurate survival prediction from histopathology images is critical for personalized cancer care, guiding treatment and risk stratification. Whole-slide images (WSIs) capture rich tissue-level morphology—including tumor architecture and microenvironmental context—but their massive size and lack of localized annotations make direct modeling challenging. Patch-based multiple instance learning (MIL) has thus become the dominant paradigm, dividing each slide into smaller tiles for weakly supervised analysis.

While MIL has succeeded in cancer grading and subtyping, survival prediction requires modeling long-range dependencies and subtle morphological cues across spatially distributed tissue regions. Conventional statistical approaches such as the Cox proportional hazards model cannot capture these non-linear, high-dimensional relationships, whereas deep models often lack interpretability and spatial reasoning.

To address these challenges, we present a unified framework combining four modules: (1) Quantile-Gated Patch Selection dynamically identifies patches and retains prognostically relevant tissue regions through quantile-based filtering. (2) Graph-Guided Clustering of Relevant Patches to capture spatial morphological coherence; (3) Hierarchical Context Attention to learn both intra- and inter-cluster dependencies; and (4) expert-driven mixture of Log-logistics framework for survival distribution estimation. Together, these components enable interpretable and accurate survival prediction by jointly leveraging spatial structure, phenotype abstraction, and probabilistic outcome modeling.

2. RELATED WORK

Weakly supervised learning has been central to WSI-based survival modeling, primarily through multiple instance learning (MIL). Early models such as AB-MIL [1], CLAM [2], and DSMIL [3] used attention pooling to highlight prognostic patches but overlooked spatial context. Graph-based PatchGCN [4] captured spatial adjacency, while hierarchical transformers like HGT [5], TransMIL [6], and HIPT [7] modeled multi-scale features at high computational cost. Recent multimodal methods such as PathoGen-X [8], CoC [9], and HiLa [10] integrate histopathology with genomic, methylation, and language data, while SCMIL [11] estimates Gaussian distribution-based survival predictions. However, these approaches lack mechanisms to disentangle latent phenotypes or exploit structural coherence. Our expert-driven mixture of log-logistics module addresses this gap by integrating phenotype-aware clustering with expert-specific survival estimation, where specialized experts capture distinct features and a gating network adaptively fuses their outputs for improved interpretability.

3. METHODOLOGY

Figure 1 illustrates the overall pipeline of the proposed framework. Each Whole Slide Image (WSI) is divided into non-overlapping patches of size 224×224

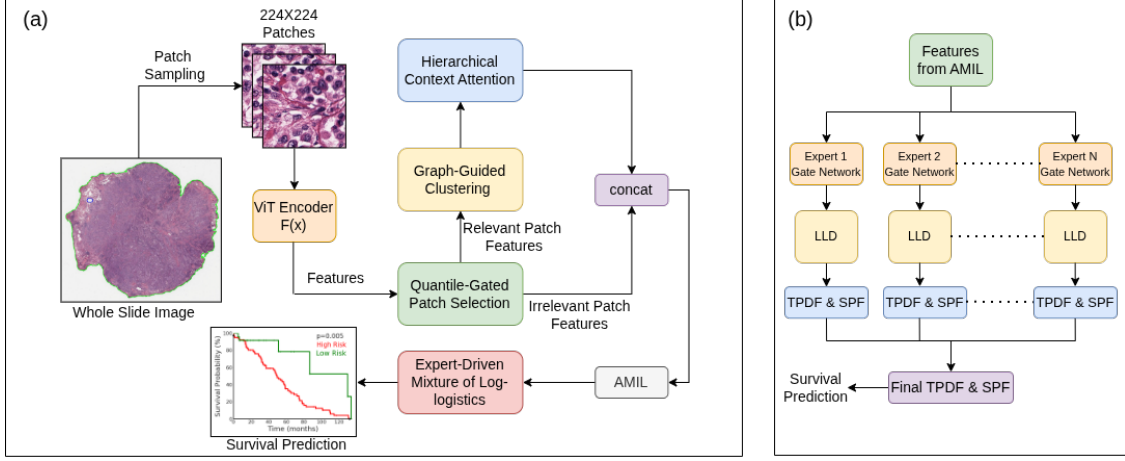


Fig. 1: (a) Proposed survival framework. (b) Expert-guided Mixture Density Modeling block.

pixels at the highest magnification level ($40\times$). Background and non-tissue regions are removed, and the remaining patches are encoded using a histopathology foundation model[12], specifically a Vision Transformer (ViT) feature extractor $F(x)$ pretrained through large-scale self-supervised learning[13] on diverse WSI datasets. This yields a patch feature matrix

$$\mathbf{P}_{\text{feat}} \in \mathbb{R}^{n \times d}, \quad (1)$$

where n denotes the number of extracted patches and d the feature dimensionality.

The proposed framework comprises four modules: Quantile-Gated Patch Selection (QGPS), Graph-Guided Clustering (GGC), Hierarchical Context Attention (HCA), and Expert-Driven Mixture of Log-logistics Module (EDMLL).

3.1. Quantile-Gated Patch Selection (QGPS)

To focus on diagnostically informative regions, a quantile-based learnable Multi Layer Perceptron (MLP) selects task-relevant patches according to their importance scores derived from model logits. For each WSI, a threshold τ_q is determined as the q -quantile of logits, retaining the top $(1 - q) \times 100\%$ of patches:

$$\mathcal{P}_{\text{sel}} = \{\mathbf{P}_i \mid \text{logit}_i > \tau_q\}, \quad \mathcal{P}_{\text{rem}} = \{\mathbf{P}_i \mid \text{logit}_i \leq \tau_q\}. \quad (2)$$

This adaptive selection removes noisy or background patches, ensuring downstream modules focus on semantically meaningful regions relevant to survival outcomes.

3.2. Graph-Guided Clustering (GGC)

The selected patches $\mathcal{P}_{\text{sel}} \in \mathbb{R}^{m \times d}$ are clustered into morphologically and spatially coherent groups. First, patch features and coordinates are normalized to comparable scales. Morphological similarity between patches is computed using cosine similarity:

$$S_{\text{morph}}(i, j) = \frac{\langle \mathbf{P}_i, \mathbf{P}_j \rangle}{\|\mathbf{P}_i\| \|\mathbf{P}_j\|}, \quad (3)$$

while spatial similarity is defined via an exponential kernel over Euclidean distances D_{ij} between normalized coordinates:

$$S_{\text{spatial}}(i, j) = \exp\left(-\frac{D_{ij}}{\sigma_D}\right), \quad \text{where } \sigma_D = \text{std}(D) + \varepsilon. \quad (4)$$

A composite similarity matrix balances both cues:

$$S = \omega_{\text{morph}} S_{\text{morph}} + \omega_{\text{spatial}} S_{\text{spatial}} \quad (5)$$

Based on S , a k -nearest-neighbor (k -NN) graph is constructed, and patches are clustered into K groups L_1, \dots, L_K using GPU-accelerated K-Means, guided by the graph structure. Each cluster represents a local tissue microenvironment such as tumor epithelium, stroma, or necrosis, promoting a biologically meaningful and spatially coherent organization across the slide.

3.3. Hierarchical Context Attention (HCA)

To capture relationships within clusters, a two-level attention mechanism is adopted.

Intra-cluster attention. Each cluster L_i undergoes multi-head self-attention (MHSA) [14] to model fine-grained local dependencies among patches:

$$L'_i = \text{LayerNorm}(L_i + \text{MHSA}(L_i)). \quad (6)$$

This step enhances contextual awareness within morphologically similar regions.

Inter-cluster attention. The refined clusters are summarized into representative embeddings

$$R_i = \frac{1}{|L'_i|} \sum_{\mathbf{x} \in L'_i} \mathbf{x}, \quad (7)$$

which are then processed by another MHSA layer to capture global relationships across regions:

$$R' = \text{LayerNorm}(R + \text{MHSA}(R)). \quad (8)$$

Intra-cluster representations are concatenated as $\tilde{P} = \text{Concat}(L'_k)_{k=1}^K$. A broadcast descriptor R'_{exp} , derived by averaging R' across clusters and expanding to match \tilde{P} , is added residually to form \hat{P} . Finally, \hat{P} is concatenated with remaining irrelevant patch features to yield $\mathcal{P}_{\text{final}}$.

WSI-level aggregation. Slide-level representation is derived via attention pooling as in AMIL [1]

$$\mathbf{z}_{\text{WSI}} = \sum_i \alpha_i \mathcal{P}_{\text{final},i}, \quad (9)$$

$$\alpha_i = \text{softmax}(W_a \tanh(W_h \mathcal{P}_{\text{final},i}^\top)),$$

where \mathbf{z}_{WSI} represents the integrated prognostic feature for the WSI.

3.4. Expert-Driven Mixture of Log-logistics (EDMLL)

An Expert-Driven Mixture of Log-logistics module (Figure 1b) is employed to estimate continuous survival probabilities by modeling the full survival time distribution. Built on the mixture-of-experts framework [15], it uses multiple experts to form Log-logistics Distributions(LLD) that capture heterogeneous survival patterns. The log-logistic probability density is given by

$$\text{LLD}(t | \alpha, \beta) = \frac{(\beta/\alpha)(t/\alpha)^{\beta-1}}{[1 + (t/\alpha)^\beta]^2}, \quad t > 0, \quad (10)$$

where $\alpha, \beta > 0$ denote the scale and shape parameters.

The survival time t of a whole slide image is directly modeled on its features derived via the attention pooling layer, as shown in Fig. 1(b). Each expert e in the mixture models the conditional distribution over t using a log-logistic mixture model (LLD):

$$p(t | \mathbf{z}_{\text{WSI}}, e) = \sum_{k=1}^K \lambda_k^{(e)}(\mathbf{z}_{\text{WSI}}) \text{LLD}(t | \alpha_k^{(e)}, \beta_k^{(e)}), \quad (11)$$

where each k component follows a log-logistic distribution with scale $\alpha_k^{(e)}$ and shape $\beta_k^{(e)}$, while mixture weights $\lambda_k^{(e)}$ are computed using a softmax over the K components. Learnable global anchors $(P_\alpha, P_\beta) \in \mathbb{R}^K$, corresponding to scale and shape parameters, are linearly projected for each expert:

$$\alpha^{(e)} = W_\alpha^{(e)} P_\alpha, \quad \beta^{(e)} = \text{softplus}(W_\beta^{(e)} P_\beta), \quad (12)$$

A gating network $G(\mathbf{z}_{\text{WSI}})$ assigns softmax weights to experts, producing the overall time probability density function (TPDF) and survival probability function (SPF) as:

$$\text{TPDF}(t | \mathbf{z}_{\text{WSI}}) = \sum_{e,k} G_e(\mathbf{z}_{\text{WSI}}) \lambda_k^{(e)} \text{LLD}(t | \alpha_k^{(e)}, \beta_k^{(e)}), \quad (13)$$

$$\text{SPF}(t | \mathbf{z}_{\text{WSI}}) = 1 - \sum_{e,k} G_e(\mathbf{z}_{\text{WSI}}) \lambda_k^{(e)} F_{\text{LLD}}(t | \alpha_k^{(e)}, \beta_k^{(e)}). \quad (14)$$

where F_{LLD} is obtained by integrating the LLD.

3.5. Training Objective and Regularization

The model is trained using a negative log-likelihood loss (\mathcal{L}_{NLL}) that handles both censored ($c = 0$ i.e. event not yet occurred) and uncensored ($c = 1$ i.e. event occurred) data. For an observed time t_d and censoring indicator $c \in \{0, 1\}$,

$$\mathcal{L}_{\text{NLL}} = -c \log(\text{TPDF}(t_d | \mathbf{z}_{\text{WSI}})) - (1-c) \log(\text{SPF}(t_d | \mathbf{z}_{\text{WSI}})) \quad (15)$$

To promote regularization, a gating entropy loss is introduced (\mathcal{L}_{ent}).

$$\mathcal{L}_{\text{ent}} = -\sum_e G_e(\mathbf{z}_{\text{WSI}}) \log(G_e(\mathbf{z}_{\text{WSI}})). \quad (16)$$

The overall loss combines the two above terms:

$$\mathcal{L}_{\text{total}} = \mathcal{L}_{\text{NLL}} + \lambda_{\text{ent}} \mathcal{L}_{\text{ent}}. \quad (17)$$

4. EXPERIMENTAL SETUP

4.1. Datasets

We evaluate the framework on three TCGA cohorts: Lung Adenocarcinoma (LUAD; 459 WSIs), Kidney Renal Clear Cell Carcinoma (KIRC; 509 WSIs), and Breast Invasive Carcinoma (BRCA; 956 WSIs) [17]. Each dataset contains WSIs annotated with overall survival time, measured in months from diagnosis to death (uncensored data, $c = 1$) or last follow-up (censored data, $c = 0$).

4.2. Training Configuration

The quantile hyperparameter is set to $q = 0.25$, retaining the top 75% of patches based on logits. Each patch in the k-NN graph connects to its 10 nearest neighbors, which are clustered into certain groups and processed by hierarchical attention with 8 heads. The Expert-Driven Mixture of Log-Logistics module employs five experts, each modeling a log-logistic distribution (LLD) with $K = 100$ components. Model is trained for 20 epochs with Adam ($\text{lr} = 2 \times 10^{-4}$, weight decay = 1×10^{-3} , dropout = 0.1) and a batch size of 1. We report mean \pm standard deviation of the Time-Dependent Concordance Index (TDC) [18] metric over 5-fold cross-validation. All experiments are conducted on an NVIDIA A6000 GPU.

5. RESULTS AND ANALYSIS

5.1. Quantitative Results

Table 1a summarizes performance across TCGA datasets. Our framework consistently achieves the highest mean TDC, indicating superior discrimination and

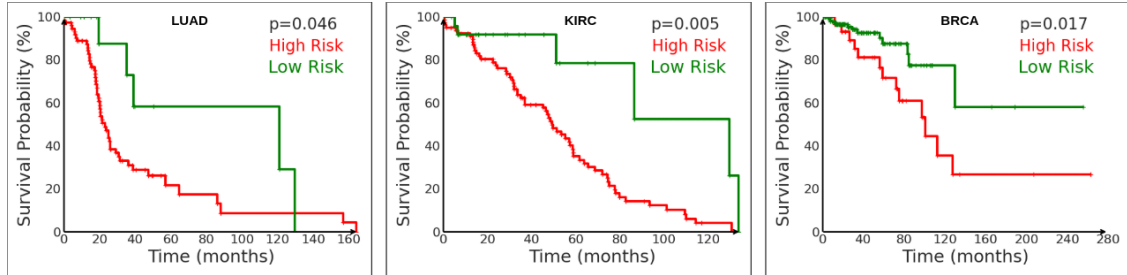


Fig. 2: Kaplan–Meier survival curves showing significant high- vs. low-risk separation across TCGA cohorts.

Table 1: Left: TCGA performance (TDC, higher is better). Right: Ablations on q in QGPS, GGC, HCA. Best TDC results in **bold**.

(a) TCGA results. Modality: I=image, G=genomic, M=methylation, L=language prompt.

Method	Modality	LUAD	KIRC	BRCA	MEAN
AMIL [1]	I	0.632 ± 0.021	0.691 ± 0.022	0.735 ± 0.013	0.686
CLAM [2]	I	0.615 ± 0.041	0.680 ± 0.028	0.652 ± 0.027	0.649
DSMIL [3]	I	0.609 ± 0.039	0.644 ± 0.013	0.668 ± 0.011	0.640
TransMIL [6]	I	0.568 ± 0.017	0.642 ± 0.076	0.636 ± 0.018	0.615
PatchGCN [4]	I	0.587 ± 0.019	0.675 ± 0.045	0.582 ± 0.037	0.615
HIPT [7]	I	0.549 ± 0.025	0.640 ± 0.037	0.625 ± 0.046	0.605
HGT [5]	I	0.607 ± 0.058	0.648 ± 0.018	0.648 ± 0.022	0.634
SCMIL [11]	I	0.622 ± 0.015	0.688 ± 0.037	0.674 ± 0.048	0.661
OTSurv [16]	I	0.638 ± 0.077	0.750 ± 0.149	0.621 ± 0.071	0.670
PathoGen-X [8]	I+G	0.620 ± 0.008	— —	0.670 ± 0.020	0.645
CoC [9]	I+M	— —	0.709 ± 0.048	0.654 ± 0.036	0.681
HiLa [10]	I+L	0.643 ± 0.055	— —	0.659 ± 0.044	0.651
Ours	I	0.644 ± 0.059	0.751 ± 0.037	0.752 ± 0.011	0.716

(b) Ablations.

Variant	LUAD	KIRC	BRCA
$q=0.5$	0.630 ± 0.022	0.738 ± 0.052	0.739 ± 0.046
$q=0.75$	0.621 ± 0.041	0.727 ± 0.037	0.729 ± 0.019
w/o QGPS	0.622 ± 0.053	0.729 ± 0.065	0.730 ± 0.027
w/o GGC, HCA	0.616 ± 0.046	0.723 ± 0.050	0.723 ± 0.011
Ours (All)	0.644 ± 0.059	0.751 ± 0.037	0.752 ± 0.011

calibration. Histology-based multiple instance learning (MIL) models—AMIL [1], CLAM [2], DSMIL [3], and TransMIL [6] served as backbones for the expert-driven mixture of log-logistics block, with performances reported for comparison. Survival-specific MIL methods such as HIPT [7], Patch-GCN [8], HGT [5], SCMIL [11] and OTSurv [16] act as baselines. Since multimodal frameworks [8, 9, 10] lack public code, their results are taken from the respective papers. By combining quantile-based patch selection, graph-guided clustering, hierarchical attention, and expert-driven mixture of log-logistics framework—each expert capturing distinct morphological or contextual cues—our model effectively identifies survival-relevant regions and achieves state-of-the-art performance on all datasets. Remarkably, it even surpasses multimodal systems while relying solely on histopathology images.

5.2. Ablation Studies and Interpretability

To assess each module’s contribution, ablation studies were performed on the Quantile-Gated Patch Selection, Graph-Guided Clustering, and Hierarchical Context Attention components (Table 1b). Varying the quantile parameter showed that $q=0.25$ offers the best trade-off, retaining prognostic regions while filtering irrelevant tissue. Removing any module causes a noticeable drop in TDC, confirming their comple-

mentary roles in denoising and spatial reasoning. For interpretability, patients were divided into high- and low-risk groups using predicted survival scores, and Kaplan–Meier (KM) curves were plotted (Fig. 2). The groups show distinct survival trends with statistically significant separation (log-rank $p=0.046$ for LUAD, $p=0.005$ for KIRC, $p=0.017$ for BRCA), validating that the expert-guided architecture captures prognostically relevant morphology. Furthermore, dynamic patch selection and graph-guided attention improve localization of high-risk regions, enhancing both predictive accuracy and clinical interpretability.

6. CONCLUSION

We proposed a unified framework for WSI-based survival prediction integrating quantile-based patch selection, graph-guided clustering, hierarchical context attention, and expert-driven mixture of log-logistics. By modeling local–global tissue interactions through clustered attention and estimating survival distributions via multiple experts, the method improves calibration and discrimination. Experiments on TCGA-LUAD, TCGA-KIRC, and TCGA-BRCA show consistent gains in time-dependent concordance over pathology-based and multimodal baselines. Future work will extend the framework toward multimodal and uncertainty-aware patient-wise survival prediction for clinical reliability.

7. COMPLIANCE WITH ETHICAL STANDARDS

This study used publicly available human data from [17]; hence, no ethical approval was required under the associated open-access license.

8. ACKNOWLEDGMENTS

The results of this study are based on the data collected from the public TCGA Research Network [17].

9. REFERENCES

- [1] Maximilian Ilse, Jakub M. Tomczak, and Max Welling, “Attention-based deep multiple instance learning,” 2018.
- [2] Ming Y. Lu, Drew F. K. Williamson, Tiffany Y. Chen, Richard J. Chen, Matteo Barbieri, and Faisal Mahmood, “Data efficient and weakly supervised computational pathology on whole slide images,” 2020.
- [3] Bin Li, Yin Li, and Kevin W. Eliceiri, “Dual-stream multiple instance learning network for whole slide image classification with self-supervised contrastive learning,” 2021.
- [4] Richard J. Chen, Ming Y. Lu, Muhammad Shaban, Chengkuan Chen, Tiffany Y. Chen, Drew F. K. Williamson, and Faisal Mahmood, “Whole slide images are 2d point clouds: Context-aware survival prediction using patch-based graph convolutional networks,” 2021.
- [5] “Multi-scope analysis driven hierarchical graph transformer for whole slide image based cancer survival prediction,” in *Medical Image Computing and Computer Assisted Intervention – MICCAI 2023*, Cham, 2023, pp. 745–754, Springer Nature Switzerland.
- [6] Zhuchen Shao, Hao Bian, Yang Chen, Yifeng Wang, Jian Zhang, Xiangyang Ji, and Yongbing Zhang, “Transmil: Transformer based correlated multiple instance learning for whole slide image classification,” 2021.
- [7] Richard J. Chen, Chengkuan Chen, Yicong Li, Tiffany Y. Chen, Andrew D. Trister, Rahul G. Krishnan, and Faisal Mahmood, “Scaling vision transformers to gigapixel images via hierarchical self-supervised learning,” 2022.
- [8] Akhila Krishna, Nikhil Cherian Kurian, Abhijeet Patil, Amruta Parulekar, Pranav Jeevan P, and Amit Sethi, “Pathogen-x: A cross-modal genomic feature trans-align network for enhanced survival prediction from histopathology images,” in *2025 IEEE 22nd International Symposium on Biomedical Imaging (ISBI)*, 2025, pp. 1–4.
- [9] Haipeng Zhou, Sicheng Yang, Sihan Yang, Jing Qin, Lei Chen, and Lei Zhu, “CoC: Chain-of-Cancer based on Cross-Modal Autoregressive Traction for Survival Prediction,” in *Medical Image Computing and Computer Assisted Intervention – MICCAI 2025*, October 2025, vol. LNCS 15974, pp. 85 – 94, Springer Nature Switzerland.
- [10] Jiaqi Cui, Lu Wen, Yuchen Fei, Bo Liu, Luping Zhou, Dinggang Shen, and Yan Wang, “HiLa: Hierarchical Vision-Language Collaboration for Cancer Survival Prediction,” in *Medical Image Computing and Computer Assisted Intervention – MICCAI 2025*, October 2025, vol. LNCS 15964, pp. 240 – 250, Springer Nature Switzerland.
- [11] Zekang Yang, Hong Liu, and Xiangdong Wang, *SCMIL: Sparse Context-Aware Multiple Instance Learning for Predicting Cancer Survival Probability Distribution in Whole Slide Images*, p. 448–458, Springer Nature Switzerland, 2024.
- [12] Mingu Kang, Heon Song, Seonwook Park, Donggeun Yoo, and Sérgio Pereira, “Benchmarking self-supervised learning on diverse pathology datasets,” 2023.
- [13] Xinlei Chen, Saining Xie, and Kaiming He, “An empirical study of training self-supervised vision transformers,” 2021.
- [14] A. et al. Vaswani, “Attention is all you need,” in *Advances in Neural Information Processing Systems*, 2017.
- [15] Christopher M. Bishop, *Pattern Recognition and Machine Learning*, Springer, New York, 2006.
- [16] Qin Ren, Yifan Wang, Ruogu Fang, Haibin Ling, and Chenyu You, “Otsurv: A multiple instance learning framework for survival prediction with heterogeneity-aware optimal transport,” in *MICCAI 2025*, 2025, pp. 439–449.
- [17] TCGA Research Network, “The cancer genome atlas pan-cancer analysis project,” *Nature Genetics*, vol. 45, no. 10, pp. 1113–1120, 2013.
- [18] Xintian Han, Mark Goldstein, and Rajesh Ranganath, “Survival mixture density networks,” 2022.